

# Transport phenomena in stochastic magnetic mirrors

Leonid Malyskin<sup>1</sup> and Russell Kulsrud<sup>2</sup>

*Princeton University Observatory, Princeton NJ 08544, USA*

<sup>1</sup>leonmal@astro.princeton.edu, <sup>2</sup>rkulsrud@astro.princeton.edu

October 29, 2018

## ABSTRACT

Parallel thermal conduction along stochastic magnetic field lines may be reduced because the heat conducting electrons become trapped and detrapped between regions of strong magnetic field (magnetic mirrors). The problem reduces to a simple but realistic model for diffusion of mono-energetic electrons based on the fact that when there is a reduction of diffusion, it is controlled by a subset of the mirrors, the principle mirrors. The diffusion reduction can be considered as equivalent to an enhancement of the pitch angle scattering rate. Therefore, in deriving the collision integral, we modify the pitch angle scattering term. We take into account the full perturbed electron-electron collision integral, as well as the electron-proton collision term. Finally, we obtain the four plasma transport coefficients and the effective thermal conductivity. We express them as reductions from the classical values. We present these reductions as functions of the ratio of the magnetic field decorrelation length to the electron mean free path at the thermal speed  $V_T = \sqrt{2kT/m_e}$ . We briefly discuss an application of our results to clusters of galaxies.

*Subject headings:* magnetic fields: conduction — magnetic fields: diffusion — methods: analytical — plasmas

## 1. Introduction

The problem of thermal conduction in a stochastic magnetic field is crucial for our understanding of galaxy cluster formation (Suginohara & Ostriker 1998; Cen & Ostriker 1999) and for the theory of cooling flows (Fabian 1990). It is also of great interest for the solar physics and for various questions of plasma physics. At the same time, the question: “whether electron thermal conduction is so strongly inhibited by a stochastic magnetic field in a galaxy cluster, that it can be neglected”, is a very controversial one (Rosner & Tucker 1989; Tribble 1989; Tao 1995; Pistinner & Shaviv 1996; Chandran & Cowley 1998). It is currently estimated that if the coefficient of thermal conductivity is less than 1/30 of the Spitzer value, then the time scale of the heat conduction in the cluster is more than the Hubble time (Suginohara & Ostriker 1998). Otherwise, thermal conduction is important.<sup>1</sup>

---

<sup>1</sup>This numerical estimate, 1/30 of the Spitzer value, is based on numerical simulations with limited resolution, so it is not the last word on the problem.

The problem of thermal diffusion of heat conducting electrons in a stochastic magnetic field should be divided into two separate parts because there are two separate effects that reduce diffusion in the presence of stochastic magnetic field (Pistinner & Shaviv 1996; Chandran, Cowley, & Ivanushkina 1999). The first effect is that the heat conducting electrons have to travel along tangled magnetic field lines, and as a result, they have to go larger distances between hot and cold regions of space. (In other words, the temperature gradients are weaker along magnetic field lines.) The second effect is that electrons, while they are traveling along the field lines, become trapped and detrapped between magnetic mirrors (which are regions of strong magnetic field). A trapped electron is reflected back and forth between magnetic mirrors until collisions make its pitch angle sufficiently small for the electron to escape the magnetic trap.

In this paper we concentrate on the second effect, and we derive the reduction of the effective electron thermal conduction parallel to the magnetic field lines caused by the presence of stochastic magnetic mirrors.

As is well known, a temperature gradient produces electrical current as well as heat flow. Similarly, an electric field produces heat flow as well as current. The four transport coefficients describing this are given in equation (34) and (35). The transport coefficients were first calculated by Spitzer & Härm for an unmagnetized plasma (Spitzer & Härm 1953; Cohen, Spitzer & Routly 1950). Their coefficients also apply in an uniform magnetic field for transport parallel to the field. In this paper, we show how the parallel transport coefficients can be reduced in the presence of stochastic magnetic mirrors, and we calculate their reduced values by the same kinetic approach as that of Spitzer & Härm. The reduction factors are presented in Figure 5. The reduced effective thermal conductivity (that resulting when the electric field is present to cancel the current) is given in Figure 6. Spatial diffusivity of mono-energetic electrons along the magnetic field lines is also presented in Figure 3.

First, in Section 2, we solve the kinetic equation to find the escape time  $\tau_m$  for electrons trapped between two equal magnetic mirrors. We assume, that all electrons have a single value of speed,  $V$ , i.e. they are mono-energetic. The exact calculations of the escape time are given in Appendices A and B. In addition, we carry out Monte-Carlo particle simulations to confirm our results.

Second, in Section 3, we apply our results for this escape time to find the reduction of diffusion of mono-energetic electrons in a system of stochastic mirrors. It turns out that in the limit  $l_0 \gg \lambda$ , where  $l_0$  is the magnetic field decorrelation length and  $\lambda$  is the electron mean free path, the parallel diffusivity is unaffected by magnetic mirrors, and is given by the standard value  $D_0 = (1/3)V\lambda$ . In the opposite limit,  $l_0 \ll \lambda$ , magnetic mirrors do reduce diffusivity. We find that in this case there is a subset of the mirrors, the principle mirrors, that inhibits diffusion the most. These are mirrors whose separation distances are approximately equal to the electron *effective mean free path*,  $\lambda_{\text{eff}}$ , the typical distance that electrons travel in the loss cones before they are scattered out of them. In order to estimate the reduction of diffusion in this limit, we need consider only the principle mirrors, neglecting all others. Again, we perform the numerical simulations to support these theoretical results.

Third, in Section 4, in order to carry out a precise kinetic treatment involving all electrons, we consider the diffusion reduction to be equivalent to an enhancement of the pitch angle scattering

rate of electrons. In deriving the collision integral, we, therefore, modify the pitch angle scattering term by the inverse of the factor by which the spatial diffusion is reduced. We take into account the full perturbed electron-electron collision integral, as well as the electron-proton collision term. We obtain an integro-differential equation for the perturbed electron distribution function in the presence of stochastic magnetic mirrors. If there is no reduction of electron diffusivity, our equation reduces to the well known result obtained by Spitzer and Härm (Spitzer & Härm 1953; Cohen, Spitzer & Routly 1950; Spitzer 1962).

Fourth, in Section 5, we solve our equation numerically, separately for the Lorentz gas in the presence of magnetic mirrors, neglecting electron-electron collisions (in this case the equation simplifies greatly), and for the Spitzer gas in the presence of magnetic mirrors. We find the reductions of the four plasma transport coefficients and of the effective thermal conductivity as functions of the ratio of the magnetic field decorrelation length  $l_0$  to the electron mean free path at the thermal speed  $V_T = \sqrt{2kT/m_e}$  (this mean free path is different for the Lorentz and Spitzer models). We find that the major effect of the magnetic mirrors is the reduction of anisotropy of superthermal electrons (this anisotropy is driven by a temperature gradient or/and by an electric field). Electrical current and heat are mainly transported by these electrons, whose diffusivity is suppressed the most.

Finally, we discuss our results and give the conclusions in Section 6.

## 2. Mono-energetic electrons trapped between two equal magnetic mirrors

In this section we solve the kinetic equation to find the escape time  $\tau_m$  for electrons trapped between two equal magnetic mirrors. We assume here and in the next section that all electrons have a single value of speed,  $V$ , which is unchanged by collisions, i.e. electrons are mono-energetic. In order to derive an analytical solution, we make several additional simplifying assumptions. Let the two magnetic barriers (mirrors) be both equal to  $B_m$ , and we assume the magnetic field  $B$  is constant between them. We introduce the *mirror strength*  $m \stackrel{\text{def}}{=} B_m/B$ . The separation of the mirrors is  $l_m$ , and their thicknesses are negligible compared to  $l_m$ . In other words, magnetic mirrors are similar to thin step-functions with heights  $B_m - B$  and with constant field  $B$  between them (see Figure 1). This is a reasonable assumption, because as we will see in the next section, electron diffusion is controlled by strong mirrors with mirror strengths  $m \gtrsim 4$ , which are separated by distances much larger than the magnetic field decorrelation length (if the spectrum of mirrors falls off with their strength significantly faster than  $1/m$ , the case that we consider in this paper).

Under these assumptions, the kinetic equation for the distribution function  $f(t, x, \mu)$  of mono-energetic electrons trapped between the two mirrors is (Braginskii 1965)

$$\frac{\partial f}{\partial t} + \mu V \frac{\partial f}{\partial x} = \frac{\nu}{2} \frac{\partial}{\partial \mu} \left[ (1 - \mu^2) \frac{\partial f}{\partial \mu} \right]. \quad (1)$$

Here  $x$  is one-dimensional space coordinate along a magnetic flux tube,  $t$  is time,  $\mu = \cos \theta$  is the cosine of the electron's pitch angle, and  $\nu = V/\lambda$  is the collision frequency [ $\lambda$  is the mean free path, see equations (43) and (46)]. The right-hand side of equation (1) represents the pitch angle scattering rate,  $\nu$ , of electrons. The electrons are trapped in the region of space between

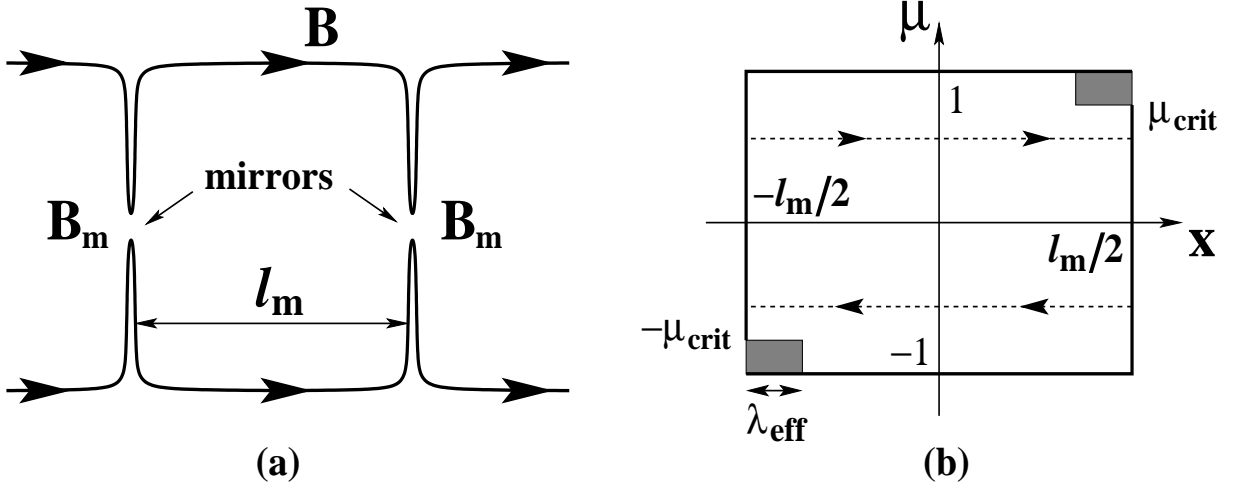


Fig. 1.— (a): A magnetic flux tube with two “step-function like” magnetic mirrors. The mirror strengths are  $m = B_m/B$ . (b): The phase space box where electrons are trapped in coordinates  $x$  and  $\mu = \cos \theta$ . The horizontal dotted lines show a closed trajectory of a trapped electron in the limit  $l_m \ll \lambda$ . The electrons escape the magnetic trap through two escape windows:  $x = l_m/2$ ,  $\mu > \mu_{\text{crit}} = \sqrt{1 - 1/m}$  and  $x = -l_m/2$ ,  $\mu < -\mu_{\text{crit}}$ . In the limit  $l_m \ll \lambda_{\text{eff}}$  the electrons freely escape to the right or left whenever they reach the two loss cones,  $\mu > \mu_{\text{crit}}$  and  $\mu < -\mu_{\text{crit}}$ . In the opposite limit,  $\lambda_{\text{eff}} \ll l_m$ , the electrons escape when they reach the two shaded regions of the phase space.

the mirrors,  $-l_m/2 < x < l_m/2$ , and they can escape through the two windows:  $x = l_m/2$ ,  $\mu > \mu_{\text{crit}} = \sqrt{1 - 1/m}$  and  $x = -l_m/2$ ,  $\mu < -\mu_{\text{crit}}$ , as shown in Figure 1. The mirror strength is  $m = B_m/B$ , and it is the measure of the relative heights of the magnetic barriers. For simplicity, we assume that the barriers are high, i.e.  $m \gg 1$  and  $\mu_{\text{crit}} \approx 1 - 1/2m$ . In this case the electron distribution is in quasi-static equilibrium,

$$f(t, x, \mu) = e^{-t/\tau_m} F(x, \mu), \quad \tau_m \gg \nu^{-1}, \quad (2)$$

and equation (1) reduces to

$$-\frac{F}{\tau_m} + \mu V \frac{\partial F}{\partial x} = \frac{\nu}{2} \frac{\partial}{\partial \mu} \left[ (1 - \mu^2) \frac{\partial F}{\partial \mu} \right]. \quad (3)$$

Let us consider an electron traveling in the loss cone  $\mu > \mu_{\text{crit}} = \sqrt{1 - 1/m} \approx 1 - 1/2m$  (or  $\mu < -\mu_{\text{crit}}$ ). The effective electron mean free path, which is the typical distance the electron travels before it is scattered by small angle collisions out of the loss cone, is

$$\lambda_{\text{eff}} \stackrel{\text{def}}{=} \lambda/2m \ll \lambda. \quad (4)$$

In other words,  $\lambda_{\text{eff}}$  is a decay distance for a flow of electrons traveling in the loss cones. The solution of equation (3) and, therefore, the escape time  $\tau_m$ , depends on the mirror strength  $m$  and the ratio  $l_m/\lambda$ . There are three limiting cases for which simple approximate solutions exist: (1)

$l_m \ll \lambda_{\text{eff}} = \lambda/2m$ ; (2)  $\lambda_{\text{eff}} \ll l_m \ll \lambda^2/\lambda_{\text{eff}} = 2m\lambda$ ; and (3)  $\lambda^2/\lambda_{\text{eff}} \ll l_m$ . We solve equation (3) for case (1) in Appendix A and for cases (2) and (3) in Appendix B, and we obtain the electron escape times

$$\begin{aligned} \tau_m^{(1)} &= \nu^{-1} \ln m, & l_m &\ll \lambda_{\text{eff}}, \\ \tau_m^{(2)} &= \nu^{-1}(l_m/\lambda_{\text{eff}}) = \nu^{-1}(2ml_m/\lambda), & \lambda_{\text{eff}} &\ll l_m \ll \lambda^2/\lambda_{\text{eff}}, \\ \tau_m^{(3)} &= \nu^{-1}(3/\pi^2)(l_m/\lambda)^2, & \lambda^2/\lambda_{\text{eff}} &\ll l_m. \end{aligned} \quad (5)$$

The following simple physical arguments help to understand these results in these three limiting cases. The collisional scattering is a two-dimensional random walk of a unit vector (which is the direction of the electron velocity) on a surface of a unit-radius sphere with frequency  $\nu$  (so, the scattered angle  $\Delta_s = \sqrt{2\nu t}$  after time interval  $t$ ). The right hand side of the kinetic equation (1) represents a one-dimensional random walk in  $\mu$ -space that follows from the two-dimensional walk because of symmetry. However, it is convenient for the moment to return to the original two-dimensional scattering because it is isotropic. The angular sizes of the two loss cones on the unit-radius sphere are  $\Delta_{\text{esc}} \approx 1/\sqrt{m}$ . First, in the limit  $l_m \ll \lambda_{\text{eff}}$ , collisions are very weak, and the scattered angle over the travel time between mirrors,  $l_m/V$ , is  $\sim \sqrt{l_m/\lambda} \ll \Delta_{\text{esc}}$ . Therefore, in this case we can disregard the electron motion in  $x$ -space. We divide the surface of the unit-radius sphere into  $\sim m$  boxes, each of angular size  $\sim \Delta_{\text{esc}} \approx 1/\sqrt{m}$ . The time it takes for the unit vector to random walk from one box to another is  $\sim \nu^{-1}/m$ , resulting in the total escape time  $\tau_m \sim m \times (\nu^{-1}/m) = \nu^{-1}$ . Because the unit vector can “visit” each box more than once, the exact result contains the logarithm of  $m$ . Second, in the limit  $\lambda_{\text{eff}} \ll l_m \ll \lambda^2/\lambda_{\text{eff}}$ , we have to consider motion in  $x$ -space as well. In this case the electrons move in three-dimensional phase space, and they escape when they are in the two loss cones within distance  $\lambda_{\text{eff}}$  from the mirrors, as shown by the shaded regions in Figure 1(b). We divide the three-dimensional phase space into  $\sim (l_m/\lambda_{\text{eff}})(1/\Delta_{\text{esc}}^2) \sim m^2 l_m/\lambda$  boxes, each of size  $\lambda_{\text{eff}} \Delta_{\text{esc}}^2 \sim \lambda/m^2$ . The time it takes to move from one box to another is  $\sim \nu^{-1}/m$ , resulting in the total escape time  $\tau_m \sim (m^2 l_m/\lambda) \times (\nu^{-1}/m) = \nu^{-1}(ml_m/\lambda)$ . Note, that the electron distribution function is almost constant in the phase space in this case (see Appendix B). Third, in the limit  $\lambda^2/\lambda_{\text{eff}} \ll l_m$ , the escape of electrons is controlled by slow diffusion in  $x$ -space, so the escape time is approximately equal to the time of diffusion between mirrors,  $\tau_m \sim \nu^{-1}(l_m/\lambda)^2$  in this case.

In our further calculations we use a simple interpolation formula

$$\tau_m \approx \tau_m^{(1)} + \tau_m^{(2)} + \tau_m^{(3)} = \nu^{-1} \left[ \ln m + (l_m/\lambda_{\text{eff}}) + (3/\pi^2)(l_m/\lambda)^2 \right] \quad (6)$$

for the whole range of parameters  $m$  and  $l_m/\lambda$ . This formula is suggested by the numerical simulations shown in Figure 2. The dots in this figure show the results of our Monte-Carlo particle simulations for three mirror strengths  $m = 2$ ,  $m = 16$  and  $m = 128$ . To obtain these results we followed  $10^3$ – $10^6$  electrons trapped between two equal magnetic mirrors separated by distance  $l_m$  ranging from  $1/1024$  to  $256$  in units of the mean free path  $\lambda$ . Independently of the initial distribution of electrons, the number of trapped electrons tends to an exponential dependence on time with the characteristic decay time  $\tau_m$  in just a few collision times [see equation (2)]. The solid lines in the figure represent formula (6) and are in a very good agreement with the simulations even for the smallest mirror strength  $m = 2$ .

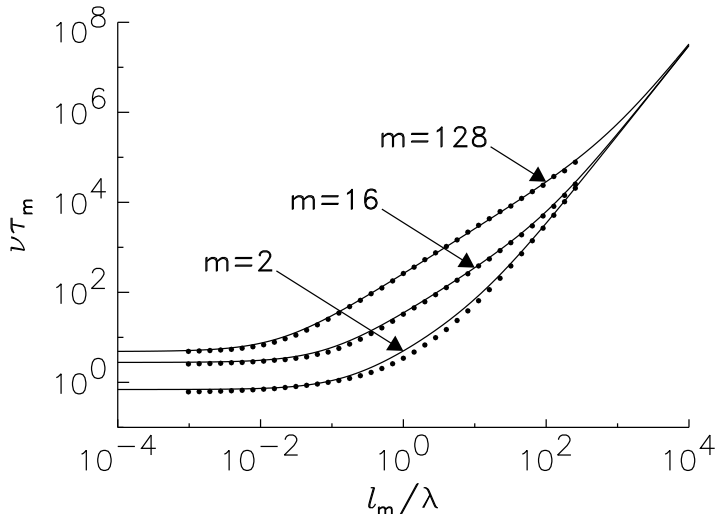


Fig. 2.— The dots show a logarithmic plot of the numerically obtained electron escape time  $\tau_m$  in units of the collision time  $\nu^{-1}$  as a function of the separation  $l_m$  of two equal magnetic mirrors in units of the mean free path  $\lambda$ . These results are based on our Monte-Carlo particle simulations of  $10^3$ – $10^6$  trapped electrons, assuming three values of the mirror strengths,  $m = 2$ ,  $m = 16$  and  $m = 128$ . The solid lines represent the analytical result, equation (6).

### 3. Diffusion of mono-energetic electrons in a system of random magnetic mirrors

In this section we continue to assume that electrons have a single value of speed,  $V$ . If there were no magnetic mirrors and the magnetic field had constant strength along the field lines, the parallel diffusion of mono-energetic electrons would be the standard spatial diffusion,  $D_0 = (1/3)V\lambda$ . Here,  $\lambda$  is the electron mean free path at speed  $V$ . However, as we have discussed in the introductory section, diffusing electrons move along flux tubes with random magnetic field strength and become trapped and detrapped between magnetic mirrors. These mirrors are regions of strong field and are separated by a field decorrelation length  $l_0$ . As a result, the diffusion is reduced by a factor that depends on the ratio  $l_0/\lambda$ .

In the main part of this section we derive this diffusion analytically and at the end of the section confirm it with numerical simulations. (In contrast to the previous section, where there were only two equal mirrors, in this section, we consider many mirrors with random spacing and strength.)

Consider the limit  $l_0 \gg \lambda$  first. In this case collisions are strong, and according to the third formula in equation (5), the time it takes for electrons to escape a trap between two magnetic mirrors is independent of the mirror strengths and is entirely controlled by the standard spatial diffusion transport of electrons between the mirrors. As a result, magnetic mirrors can be ignored, and there is no reduction of diffusion;  $D = D_0$ .

In the opposite limit,  $l_0 \ll \lambda$ , the collisions are weak, and magnetic mirrors do result in a reduction of diffusion. To find this reduction, we divide all mirrors into equal size bins  $b_m =$

$(m - \delta/2, m + \delta/2]$ , where  $m$  is the bin central mirror strength, and constant  $\delta$  is the width of the bins (the value of  $\delta$  will be discussed later).

For the moment we consider the diffusion in the presence of only those mirrors that are in a single bin  $b_m$ . It turns out that one of the bins leads to a smaller diffusion than any other bin, and the net diffusion due to all the mirrors is approximately that due to only mirrors in this bin, provided that the bins are sufficiently wide.

Let the spectrum of magnetic mirror strengths be  $\mathcal{P}(m)$ . We assume that strong magnetic mirrors are rare, i.e. the spectrum falls off fast with the mirror strength (we will estimate how fast it should fall off, below). The probability that a mirror belongs to bin  $b_m$  is

$$p_m = \int_{m-\delta/2}^{m+\delta/2} \mathcal{P}(m') dm' \approx \delta \mathcal{P}(m) + (\delta^3/24)\mathcal{P}''(m). \quad (7)$$

At each decorrelation length  $l_0$  the magnetic field changes and becomes decorrelated. Therefore, the mean separation of mirrors that are in bin  $b_m$  is

$$l_m = l_0 \sum_{k=1}^{\infty} k p_m (1 - p_m)^{k-1} = l_0/p_m. \quad (8)$$

Let us consider an electron trapped between two mirrors of bin  $b_m$ . The time  $\tau_m$  that it takes for this electron to escape the trap is given by equation (6), where we keep only the first two terms (because  $l_0 \ll \lambda$ )

$$\tau_m \approx \tau_m^{(1)} + \tau_m^{(2)} = \nu^{-1} \ln(mq_m). \quad (9)$$

Here, we introduce the important parameter

$$q_m \stackrel{\text{def}}{=} \exp(l_m/\lambda_{\text{eff}}) = \exp(2ml_0/p_m\lambda), \quad (10)$$

where the mean distance  $l_m$  between the two mirrors is given by equation (8). After the electron escapes, it travels freely in the loss cone in one of the two directions along the magnetic field lines until it is again trapped between another two mirrors of bin  $b_m$ . The freely traveling electron becomes first trapped with probabilities  $1 - e^{-l_m/\lambda_{\text{eff}}} = 1 - q_m^{-1}$  in  $0 \leq x < l_m$ ,  $e^{-l_m/\lambda_{\text{eff}}} - e^{-2l_m/\lambda_{\text{eff}}} = q_m^{-1} - q_m^{-2}$  in  $l_m \leq x < 2l_m$ ,  $e^{-2l_m/\lambda_{\text{eff}}} - e^{-3l_m/\lambda_{\text{eff}}} = q_m^{-2} - q_m^{-3}$  in  $2l_m \leq x < 3l_m$ , and so on. Therefore, the mean distance squared  $\langle \Delta x^2 \rangle_m$  that the electron travels in the loss cones before trapping is

$$\langle \Delta x^2 \rangle_m \approx l_m^2 \sum_{k=1}^{\infty} k^2 (q_m^{-k+1} - q_m^{-k}) = l_m^2 \frac{q_m(q_m + 1)}{(q_m - 1)^2}. \quad (11)$$

The processes of trapping and detrapping repeat in time intervals  $\tau_m$ . In other words, electrons random walk along the field lines in a system of mirrors that belong to bin  $b_m$  with steps  $\approx \langle \Delta x^2 \rangle_m$  in time intervals  $\approx \tau_m$ . As a result, the diffusion coefficient for these electrons is  $D(m) = C [\langle \Delta x^2 \rangle_m / 2\tau_m]$ , where we introduce a scaling constant  $C$ , which is of the order unity and will be determined by the numerical simulations. The corresponding reduction of diffusion is

$$D(m)/D_0 = C \frac{3}{2} \left( \frac{l_0}{\lambda} \right)^2 \frac{q_m(q_m + 1)}{(q_m - 1)^2} \frac{1}{p_m^2} \frac{1}{\ln(mq_m)}, \quad l_0 \ll \lambda, \quad (12)$$

where we use  $D_0 = (1/3)\nu\lambda^2$  and equations (8), (9) and (11);  $p_m$  and  $q_m$  are given by equations (7) and (10).

For a given spectrum of mirrors  $\mathcal{P}(m)$  and given constants  $\delta$  and  $C$ , the diffusion reduction (12) due to mirrors of bin  $b_m$ , is a function of mirror strength  $m$ . Let us analyze this function in two limits:  $\ln q_m \ll 1$  and  $\ln q_m \gg \ln m \gtrsim 1$ . If  $\ln q_m \ll 1$ , then  $q_m - 1 = 2ml_0/p_m\lambda \ll 1$ . Therefore,  $D(m)/D_0 \approx C(3/4)(1/m^2 \ln m)$  and  $(d/dm)[D(m)/D_0] < 0$ . On the other hand, if  $\ln q_m \gg \ln m$ , then  $D(m)/D_0 \approx C(3/4)(l_0/\lambda)(1/mp_m)$ . Therefore,  $(d/dm)[D(m)/D_0] > 0$  if the spectrum of mirrors falls off faster than  $1/m$  with the mirror strength.<sup>2</sup> In this paper we make an assumption that the spectrum falls off significantly faster than  $1/m$ .

Therefore, a minimum of  $D(m)/D_0$  exists. Let this minimum be achieved at  $m = m_p$ . Then  $\ln q_{m_p} = l_{m_p}/\lambda_{\text{eff}} \sim 2/\ln m_p \sim 1$ , or  $l_{m_p} \sim \lambda_{\text{eff}}$ . The minimum can roughly be estimated as  $D(m_p)/D_0 = \min \{D(m)/D_0\} \sim 1/m_p^2$ , which is in agreement with the qualitative results of Albright *et al.* (2000).

In other words, if  $l_0 \ll \lambda$ , then there is the bin that inhibits diffusion the most. We call it the principle bin,  $b_p = (m_p - \delta/2, m_p + \delta/2]$ . The corresponding mirror strength  $m_p$  is the principle mirror strength. The minimum of diffusion  $D(m)$  due to mirrors of bin  $b_m$  is achieved at the principle strength,  $m = m_p$ . The spacing of mirrors that are in the principle bin is of the order of the effective mean free path for this bin,  $l_{m_p} \sim \lambda_{\text{eff}} = \lambda/2m_p$ . The main idea is that, in order to estimate the net diffusion due to all mirrors, we need consider only magnetic mirrors that are in the principle bin and we can neglect all other bins. Mirrors that are smaller than the principle mirrors “work” poorly in the inhibition of diffusion because they are weak and are separated by distances less than  $\lambda_{\text{eff}}$  (which is the distance that electrons travel in the loss cones). Mirrors that are larger than the principle mirrors “work” poorly, because they are very rare and are separated by very large distances (provided the mirror spectrum falls off with the mirror strength significantly faster than  $1/m$ ). These assumptions are supported by our numerical simulations (see Figure 3).

As a result of these considerations, we can combine our theoretical results for the reduction of diffusion of mono-energetic electrons,  $R_D = D/D_0$ , into a single formula valid in the two limits for  $l_0/\lambda$ :

$$R_D = D/D_0 = \begin{cases} \min_m \{D(m)/D_0\} = D(m_p)/D_0, & l_0 \ll \lambda, \\ 1, & l_0 \gg \lambda, \end{cases} \quad (13)$$

where  $D(m)/D_0$  is given by equation (12), and the minimum is achieved at the principle mirror strength  $m = m_p$  (note that  $\ln q_{m_p} = l_{m_p}/\lambda_{\text{eff}} \sim 1$ ).

We show the theoretical mono-energetic diffusion reduction (13) by the solid lines in Figure 3

---

<sup>2</sup>This criterion is different from the result of Albright *et al.* (2000), who found  $1/m^2$  to be the boundary spectrum for the transition between their diffusive and subdiffusion regimes. We believe that the difference arises because, for flat spectra, our bin width  $\delta$  starts to depend on  $l_0/\lambda$  (and our simple diffusion model breaks down).



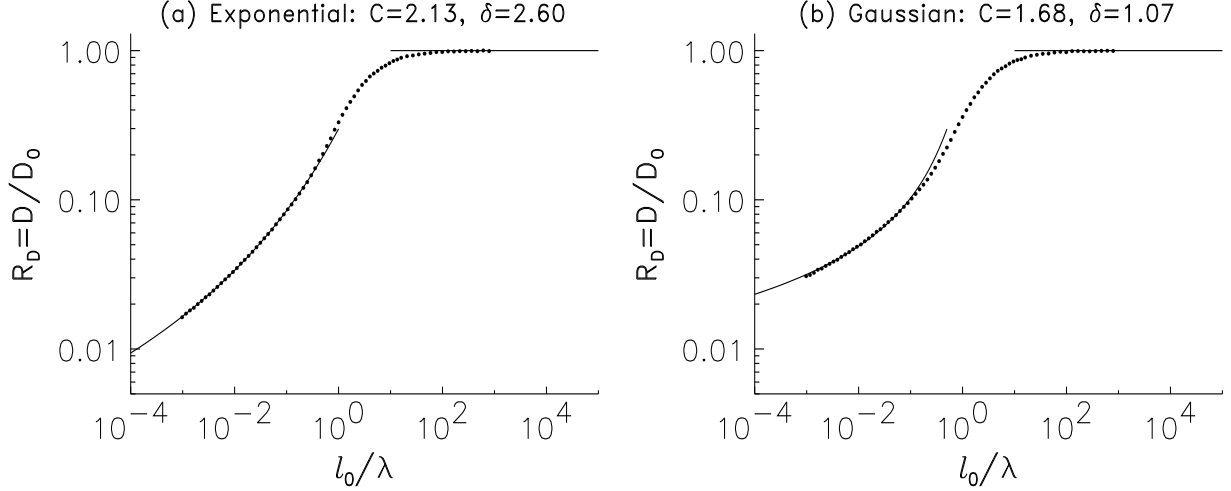


Fig. 3.— We consider two mirror spectra: (a) exponential, and (b) Gaussian [see eqs. (14)]. The dots show the reduction of diffusion,  $R_D = D/D_0$ , obtained by Monte-Carlo particle simulations of  $1\text{--}6 \times 10^5$  electrons, each followed in a system of magnetic mirrors over 300 collision times  $\nu^{-1}$ . The solid lines represent the theoretical results given by equation (13). The constants  $C$  and  $\delta$  are obtained by matching the theoretical results with the results of simulations for each of the two spectra (and these constants do not depend on  $l_0/\lambda$ ).

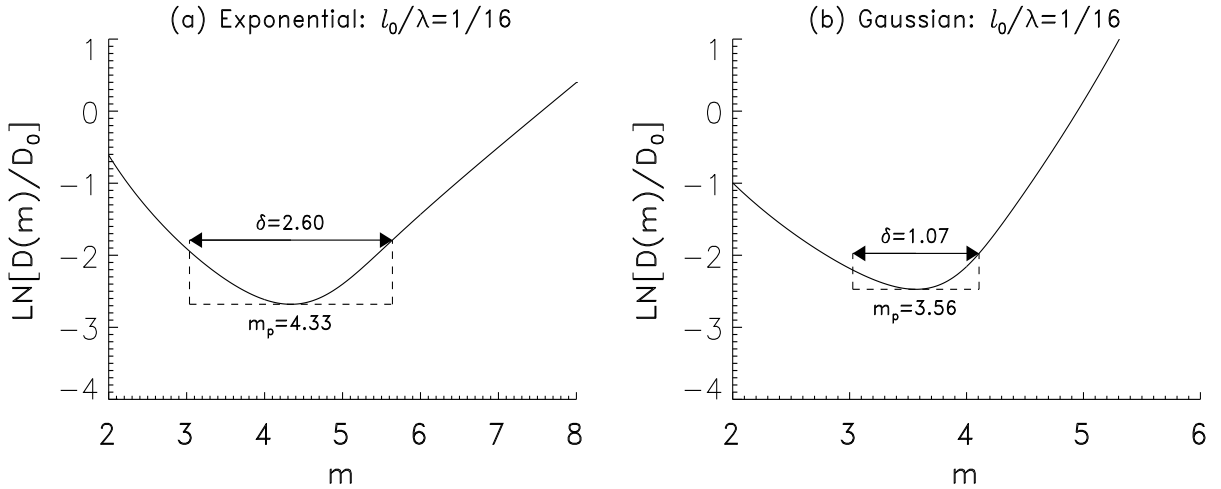


Fig. 4.— The natural logarithm of the diffusion reduction (12) caused by mirrors that are in bin  $b_m$  for  $l_0/\lambda = 1/16$ . We consider two mirror spectra: (a) exponential, and (b) Gaussian [see eqs. (14)]. The principle bins are shown by arrows. In case of each spectrum, the reduction has the minimum at the principle mirror strength  $m_p$ , and it roughly doubles at the boundaries of the principle bin.

for two mirror spectra: exponential and Gaussian<sup>3</sup>,

$$\begin{aligned}\mathcal{P}(m) &= e^{-(m-2)} \text{ exponential,} \\ \mathcal{P}(m) &= (2/\pi)^{1/2} e^{-(m-2)^2/2} \text{ Gaussian.}\end{aligned}\tag{14}$$

The results of our Monte-Carlo particle simulations are shown by dots. The constants  $C$  and  $\delta$  (shown at the top) are of the order unity, and we adjust them by matching our theoretical results with the results of simulations in case of each of the two spectra ( $C$  and  $\delta$  do not depend on  $l_0/\lambda$ ). The simulations are based on  $1-6 \times 10^5$  particles. For each particle we choose a distribution of mirrors  $m \geq 2$ , which all are separated by the magnetic field decorrelation length  $l_0$ , and are chosen according to the assumed mirror spectrum (14). We follow the particles during 300 collision times  $\nu^{-1}$ . Then we average the particle displacements squared  $\langle \Delta x^2 \rangle$  at a given time  $t$  to obtain the diffusion coefficient  $\langle \Delta x^2 \rangle / 2t$  given in Figure 3.

Note that the bin width  $\delta$  is larger for the exponential spectrum than it is for the Gaussian. This is because the later is steeper at large mirror strengths. Figures 4(a) and 4(b) clearly demonstrate the difference. In these figures we plot the natural logarithm of the diffusion reduction (12) caused by mirrors that are in bin  $b_m$  versus the mirror strength  $m$  for  $l_0/\lambda = 1/16$  and for the both spectra (14) of mirror strengths. The principle bins are shown by arrows. In case of each spectrum, the reduction has the minimum at the corresponding principle mirror strength  $m_p$ . We see, that the reduction roughly doubles over its minimal value at the boundaries of the principle bin,  $m = m_p + \delta/2$  and  $m = m_p - \delta/2$ .

#### 4. The Fokker-Planck kinetic equation

In this section we use the results found above to obtain the modified kinetic equation for electrons traveling in a system of random magnetic mirrors. The reduction of diffusion of mono-energetic electrons with speed  $V$ ,  $R_D$ , obtained in the previous section can be considered to be equivalent to an enhancement of the pitch angle scattering rate, since the pitch angle scattering is directly related to spatial diffusion. We therefore, in deriving the collision integral, modify the pitch angle scattering term by factor  $R_D^{-1}$ , where  $R_D$  is the factor by which the spatial diffusion is reduced (see the previous section). Hereafter, we do not assume electrons to be mono-energetic. We take into account the full perturbed electron-electron collision integral, as well as the electron-proton collision term. When  $R_D \equiv 1$ , our equations reduce to those of Spitzer and Härm in their well known paper (Spitzer & Härm 1953; Cohen, Spitzer & Routly 1950; Spitzer 1962).

The electron distribution function is

$$f(\mu, V) = f_0(V) + f_1(\mu, V),\tag{15}$$

where  $f_0$  is the zero order isotropic part given by the Maxwellian distribution,

$$f_0 = n(x) [m_e/2\pi kT(x)]^{3/2} e^{-m_e V^2/2kT(x)} = n\pi^{-3/2} V_T^{-3} e^{-v^2},\tag{16}$$

---

<sup>3</sup>We find the minimum in equation (13) numerically.

and  $f_1 \propto \mu$  is the first order anisotropic perturbation (of order the temperature gradient and electric field)

$$f_1(\mu, V) = \mu n V_T^{-3} S(v). \quad (17)$$

Here  $m_e$  is the electron mass,  $k$  is the Boltzmann constant, and the electron temperature  $T(x)$  and concentration  $n(x)$  slowly change in space. We also introduce the dimensionless electron speed  $v = V/V_T$ , where the thermal electron speed is  $V_T = \sqrt{2kT/m_e}$ . Thus, the function  $S(v)$  in equation (17) is dimensionless.

In a steady state, the kinetic equation for the electrons is obviously

$$V_x(\partial f_0/\partial x) - (eE/m_e)(\partial f_0/\partial V_x) = (\delta f/\delta t)_c, \quad (18)$$

where  $(\delta f/\delta t)_c$  is the Coulomb collision integral that includes electron-proton and electron-electron collisions,  $V_x = \mu V$  is the  $x$ -component of the electron velocity (the component along the magnetic field lines), and  $E$  is the electric field in the  $x$ -direction. The electron pressure should be constant,  $P = k n(x)T(x) = \text{const.}$ <sup>4</sup> As a result, the derivatives of the Maxwellian electron distribution are

$$\partial f_0/\partial x = (v^2 - 2.5)(f_0/T)(dT/dx), \quad \partial f_0/\partial V_x = -(2\mu/V_T)v f_0. \quad (19)$$

The collision integral is divided up as

$$(\delta f/\delta t)_c = (\delta f_0/\delta t)_0 + (\delta f_1/\delta t)_0 + (\delta f_0/\delta t)_1 = (\delta f_1/\delta t)_0 + (\delta f_0/\delta t)_1, \quad (20)$$

where  $(\delta f_0/\delta t)_0 \equiv 0$  corresponds to Maxwellian collisions acting on  $f_0$ ,  $(\delta f_1/\delta t)_0$  corresponds to Maxwellian collisions (with enhanced pitch angle scattering) acting on  $f_1$ , and  $(\delta f_0/\delta t)_1$  corresponds to perturbed collisions acting on  $f_0$  (since  $f_0$  is isotropic, there is no pitch angle scattering in this collision term). The collision integral (20) can be best obtained, in the Fokker-Planck form, by using the Rosenbluth potentials  $h(\mu, V) = h_0(V) + h_1(\mu, V)$  and  $g(\mu, V) = g_0(V) + g_1(\mu, V)$  (Rosenbluth, MacDonald, & Judd 1957). Here  $h_0$  and  $g_0$  are calculated using the Maxwellian parts of the electron and ion distribution functions (16), while the perturbed potentials,  $h_1 = 2\mu\mathcal{A}_1(V)$  and  $g_1 = \mu\mathcal{B}_1(V)$ , are proportional to  $\mu$ , and they are calculated using the perturbed part of the electron distribution function (17).

The Maxwellian potentials  $h_0$  and  $g_0$  determine the  $(\delta f_1/\delta t)_0$  part of the Fokker-Planck collision integral, and the perturbed potentials,  $h_1 = 2\mu\mathcal{A}_1(V)$  and  $g_1 = \mu\mathcal{B}_1(V)$ , are used to find the  $(\delta f_0/\delta t)_1$  part of the Fokker-Planck collision integral [see the equation (31) of Rosenbluth, MacDonald, & Judd 1957]

$$\begin{aligned} (\delta f_1/\delta t)_0 &= \frac{A_D}{2n} \left\{ -\frac{1}{V^2} \frac{\partial}{\partial V} \left[ f_1 V^2 \frac{dh_0}{dV} \right] + \frac{1}{2V^2} \frac{\partial^2}{\partial V^2} \left[ f_1 V^2 \frac{d^2 g_0}{dV^2} \right] \right. \\ &\quad \left. - \frac{1}{V^2} \frac{\partial}{\partial V} \left[ f_1 \frac{dg_0}{dV} \right] + R_D^{-1} \frac{1}{2V^3} \frac{dg_0}{dV} \frac{\partial}{\partial \mu} \left[ (1 - \mu^2) \frac{\partial f_1}{\partial \mu} \right] \right\}, \end{aligned} \quad (21)$$

---

<sup>4</sup>Because the hydrodynamic time scale is much shorter than the transport, e.g thermal conduction, time scale.

$$\begin{aligned}
(\delta f_0/\delta t)_1 &= \mu \frac{A_D}{2n} \left\{ -\frac{2}{V^2} \frac{d}{dV} \left[ f_0 V^2 \frac{d\mathcal{A}_1}{dV} \right] + \frac{4}{V^2} f_0 \mathcal{A}_1 + \frac{1}{2V^2} \frac{d^2}{dV^2} \left[ f_0 V^2 \frac{d^2 \mathcal{B}_1}{dV^2} \right] \right. \\
&\quad \left. - \frac{3}{V^3} f_0 \frac{d\mathcal{B}_1}{dV} + \frac{3}{V^4} f_0 \mathcal{B}_1 - \frac{3}{V^2} \frac{d}{dV} \left[ f_0 \frac{d\mathcal{B}_1}{dV} \right] + \frac{3}{V^2} \frac{d}{dV} \left[ f_0 \frac{\mathcal{B}_1}{V} \right] \right\}. \tag{22}
\end{aligned}$$

For a hydrogen plasma the “diffusion constant”  $A_D$  is

$$A_D = 8\pi n e^4 \ln \Lambda / m_e^2, \tag{23}$$

where  $e$  is the absolute value of the electron charge, and  $\ln \Lambda$  is the Coulomb logarithm (Spitzer 1962). Note, that the last term in equation (21) is the pitch angle scattering term, and we multiply it by our enhancement factor  $R_D^{-1}$  [compare this term with the right-hand side of equation (1)].

Using the equations (17) and (18) of Rosenbluth, MacDonald, & Judd (1957), we express the derivatives of the potentials  $h_0$  and  $g_0$  in terms of the three Maxwellian diffusion coefficients  $\langle \Delta V_{\parallel} \rangle_0$ ,  $\langle (\Delta V_{\perp})^2 \rangle_0$  and  $\langle (\Delta V_{\parallel})^2 \rangle_0$ , which are further given in terms of error functions [see the equations (5-15)–(5-20) of Spitzer 1962]

$$\begin{aligned}
dh_0/dV &= (2n/A_D) \langle \Delta V_{\parallel} \rangle_0 = -(n/V^2)[1 + 4v^2 G(v)], \\
dg_0/dV &= (n/A_D)V \langle (\Delta V_{\perp})^2 \rangle_0 = n[1 + \Phi(v) - G(v)], \\
d^2 g_0/dV^2 &= (2n/A_D) \langle (\Delta V_{\parallel})^2 \rangle_0 = (2n/V)G(v).
\end{aligned} \tag{24}$$

Here  $\Phi$  is the usual error function, and  $G$  is expressed in terms of  $\Phi$  and its derivative  $\Phi'$ , they are functions of the dimensionless speed  $v = V/V_T$  [ $V_T = \sqrt{2kT/m_e}$ ],

$$\Phi(v) = (2/\sqrt{\pi}) \int_0^v e^{-x^2} dx, \quad G(v) = \frac{\Phi(v) - v\Phi'(v)}{2v^2}. \tag{25}$$

The perturbed potentials,  $h_1 = 2\mu\mathcal{A}_1(V)$  and  $g_1 = \mu\mathcal{B}_1(V)$ , are calculated using the perturbed electron distribution function (17) and are given by the following formulas [see the equations (40), (41), (45) and (46) of Rosenbluth, MacDonald, & Judd 1957]

$$\begin{aligned}
\mathcal{A}_1 &= (4\pi/3)(n/V_T) [v^{-2}\bar{I}_3(S;v) + v\underline{I}_0(S;v)], \\
\mathcal{B}_1 &= (4\pi/3)nV_T [0.2v^{-2}\bar{I}_5(S;v) - \bar{I}_3(S;v) - v\underline{I}_2(S;v) + 0.2v^3\underline{I}_0(S;v)],
\end{aligned} \tag{26}$$

where we introduce integrals

$$\bar{I}_m(S;v) = \int_0^v v^m S(v) dv, \quad \underline{I}_m(S;v) = \int_v^{\infty} v^m S(v) dv, \tag{27}$$

Now, substituting equations (16), (17), (24) and (26) into formulas (21) and (22), and using definitions (25), (27) and equation (20), after considerable algebra, we have for the collision integrals

$$\begin{aligned}
(\delta f_1/\delta t)_0 &= (nA_D/2V_T^6) \mu v^{-2} (\hat{\mathcal{L}}S - 2v^2\Phi'S), \\
(\delta f_0/\delta t)_1 &= (nA_D/2V_T^6) \mu v^{-2} (\hat{\mathcal{I}}S + 2v^2\Phi'S), \\
(\delta f/\delta t)_c &= (nA_D/2V_T^6) \mu v^{-2} (\hat{\mathcal{L}}S + \hat{\mathcal{I}}S),
\end{aligned} \tag{28}$$

where the differential and the integral operators are defined as

$$\hat{\mathcal{L}}S(v) = d/dv [vG(dS/dv)] + 2v^2G(dS/dv) - [v^{-1}R_D^{-1}(1 + \Phi - G) - 4v^2\Phi']S, \quad (29)$$

$$\hat{\mathcal{I}}S(v) = (4/15\sqrt{\pi})e^{-v^2} [12\bar{I}_5(S;v) - 10\bar{I}_3(S;v) + 2v^3(6v^2 - 5)\underline{I}_0(S;v)]. \quad (30)$$

The enhancement of the Maxwellian pitch angle scattering rate,  $R_D^{-1}$ , enters into the differential operator (29).  $R_D$  depends on the dimensionless speed  $v = V/V_T$ , we will explicitly give this dependence in equations (42) and (45).

Finally, substituting formulas (28) and (19) into equation (18), we obtain the kinetic equation for the dimensionless perturbed electron distribution function  $S(v)$  [see equation (17)]

$$\hat{\mathcal{L}}S = \gamma_T v^3(2v^2 - 5)e^{-v^2} + \gamma_E v^3 e^{-v^2} - \hat{\mathcal{I}}S, \quad (31)$$

$$S(v) \rightarrow 0, \quad \text{as } v \rightarrow 0 \text{ and as } v \rightarrow \infty, \quad (32)$$

where constants  $\gamma_T$  and  $\gamma_E$  are

$$\gamma_T = \frac{k^2 T}{2\pi^{5/2} n e^4 \ln \Lambda} \frac{dT}{dx}, \quad \gamma_E = \frac{kT}{\pi^{5/2} n e^3 \ln \Lambda} E. \quad (33)$$

We also take the obvious boundary conditions (32) for function  $S$ . Equations (29)–(31) reduce to the Spitzer equations for an ionized hydrogen gas (Spitzer & Härm 1953; Cohen, Spitzer & Routly 1950) if we set  $R_D \equiv 1$  and make a substitution  $S(v) = \pi^{-3/2} e^{-v^2} D(v)$ . However, we prefer to use function  $S$ , because of the simpler boundary conditions (32).

## 5. The reduction of transport coefficients by stochastic magnetic mirrors

In a steady state, an electric field  $E$  and a temperature gradient  $dT/dx$  both produce anisotropic perturbations of the electron distribution function,  $f_1(\mu, v) = \mu n V_T^{-3} S(v)$ , see equations (15) and (17). This anisotropy results in an electron flow and, consequently, in an electric current  $j$  and in a heat flow  $Q$  along magnetic field lines (in the  $x$ -direction)

$$j = -e \int_0^\infty \int_{-1}^1 \mu V f_1 d\mu 2\pi V^2 dV = \sigma E + \alpha (dT/dx), \quad (34)$$

$$Q = \int_0^\infty \int_{-1}^1 \mu V (m_e V^2/2) f_1 d\mu 2\pi V^2 dV = -\beta E - \kappa (dT/dx). \quad (35)$$

Here  $\sigma$ ,  $\alpha$ ,  $\beta$  and  $\kappa$  are the four transport coefficients to be found ( $\sigma$  and  $\kappa$  are the electrical and thermal conductivities).

Before we proceed to the calculation of the transport coefficients, let us first call attention to the electron flow produced by the electric field. The electric field produces two different kinds of the electron flow. The first, the main, flow is due to acceleration of electrons, which is described by the term containing  $E$  in equation (18), and correspondingly by the term containing  $\gamma_E$  in equation (31). The second, an additional, flow arises because the electric field changes the size of the two loss cones of a mirror trap, so in Figure 1(b)  $\mu_{\text{crit}}$  in the right upper corner is not equal to

$\mu_{\text{crit}}$  in the left lower corner. As a result, the electrons are more likely to escape the trap in the direction opposite to the electric field. Fortunately, this additional flow, which is rather complicated to find precisely, can be neglected compared to the flow due to acceleration. We give a prove of this in Appendix C. <sup>5</sup>

In further calculations, it is convenient to break  $S(v)$  into the two separate inhomogeneous solutions of equation (31), which we denote as  $S_T(v)$  and  $S_E(v)$ . <sup>6</sup> The first solution,  $S_T$ , is obtained by setting  $\gamma_T = 1$  and  $\gamma_E = 0$ , and the second solution,  $S_E$ , is obtained by setting  $\gamma_T = 0$  and  $\gamma_E = 1$ , i. e.

$$\begin{aligned} S_T(v) &= S(v), & \text{when } \gamma_T = 1 \text{ and } \gamma_E = 0, \\ S_E(v) &= S(v), & \text{when } \gamma_T = 0 \text{ and } \gamma_E = 1. \end{aligned} \quad (36)$$

The general solution to equation (31) and the perturbed distribution function (17) are the linear combinations of the two inhomogeneous solutions,

$$\begin{aligned} S(v) &= \gamma_T S_T(v) + \gamma_E S_E(v), \\ f_1(\mu, v) &= \mu n V_T^{-3} [\gamma_T S_T(v) + \gamma_E S_E(v)]. \end{aligned} \quad (37)$$

In other words,  $S_T$  and  $S_E$  correspond to anisotropic perturbations of the electron distribution function, which are driven by the temperature gradient and by the electric field respectively, while  $S = \gamma_T S_T + \gamma_E S_E$  is the total anisotropic perturbation.

We now consider separately two cases: first, the Lorentz gas in a system of random mirrors, and second, the Spitzer gas in a system of random mirrors. For the Lorentz gas, electrons are assumed only to collide with protons, so equations (29)–(31) become greatly simplified. For the Spitzer gas, we consider both the electron-electron the electron-proton collisions, so we solve the full set of our equations.

### 5.1. Lorentz gas in a system of random mirrors

Here we assume the electrons to collide only with protons, so we have for operators (29) and (30)

$$\hat{\mathcal{L}}S = -S/vR_D, \quad \hat{\mathcal{I}}S = 0, \quad (38)$$

resulting in the two simple inhomogeneous solutions (36) of equation (31),

$$S_T(v) = -v^4(2v^2 - 5)e^{-v^2}R_D, \quad S_E(v) = -v^4e^{-v^2}R_D. \quad (39)$$

---

<sup>5</sup>The main reason is that the difference in the two loss cones due to electric field is inversely proportional to the electron kinetic energy, so the additional flow has a factor  $1/V^2$  compared to a factor  $1/V_T^2$  that enters the main flow due to acceleration. Because both the current and the heat flow are mainly transported by superthermal electrons  $v = V/V_T \sim 2$ , the additional flow is approximately 20% of the main flow, see Appendix C.

<sup>6</sup>The two homogeneous solutions of equation (31) must be excluded, because they diverge either at  $v \rightarrow 0$  or at  $v \rightarrow \infty$ , violating the conditions (32), see more details in Cohen, Spitzer & Routly 1950.

If there are no magnetic mirrors, so  $R_D \equiv 1$ , we substitute equations (39) into formula (37) and easily carry out the two integrals in equations (34) and (35). Taking into consideration definitions (33), we obtain the well-known Lorentz transport coefficients (Spitzer 1962)

$$\begin{aligned}\sigma_L &= 2 \left(\frac{2}{\pi}\right)^{3/2} \frac{(kT)^{3/2}}{m_e^{1/2} e^2 \ln \Lambda}, & \alpha_L &= 3 \left(\frac{2}{\pi}\right)^{3/2} \frac{k(kT)^{3/2}}{m_e^{1/2} e^3 \ln \Lambda}, \\ \beta_L &= 8 \left(\frac{2}{\pi}\right)^{3/2} \frac{(kT)^{5/2}}{m_e^{1/2} e^3 \ln \Lambda}, & \kappa_L &= 20 \left(\frac{2}{\pi}\right)^{3/2} \frac{k(kT)^{5/2}}{m_e^{1/2} e^4 \ln \Lambda}.\end{aligned}\quad (40)$$

If there are magnetic mirrors, it is convenient to normalize the resulting transport coefficients to the corresponding Lorentz coefficients (40). Substituting equation (37) into the two integrals in equations (34) and (35), and again using definitions (33), we have

$$\begin{aligned}\sigma/\sigma_L &= -(1/3) \bar{I}_3(S_E; \infty), & \alpha/\alpha_L &= -(1/9) \bar{I}_3(S_T; \infty), \\ \beta/\beta_L &= -(1/12) \bar{I}_5(S_E; \infty), & \kappa/\kappa_L &= -(1/60) \bar{I}_5(S_T; \infty),\end{aligned}\quad (41)$$

where the integral moments are defined by equations (27), and  $S_T$  and  $S_E$  are given by equations (39).

In order to find explicitly the diffusion reduction factor  $R_D$  in equations (39) as a function of  $v$ , we refer to the results of Section 3. In those section we found the diffusion reduction as a function of the ratio of the magnetic field decorrelation length  $l_0$  to the electron mean free path  $\lambda$ . For Lorentz electrons the mean free path  $\lambda_L$  is proportional to the fourth power of the electron speed,  $\lambda_L \propto V^4$ , (Spitzer 1962, Braginskii 1965). Thus, we have

$$R_D = R_D(l_0/\lambda_L) = R_D(v^{-4}l_0/\lambda_{L,T}), \quad (42)$$

where  $\lambda_{L,T}$  is obviously the Lorentz electron mean free path at the thermal speed  $V_T = \sqrt{2kT/m_e}$

$$\lambda_{L,T} = (kT)^2 / \pi n e^4 \ln \Lambda \approx 0.1 \text{ Kpc } (T/10^7 \text{ K})^2 (10^{-3} \text{ cm}^{-3}/n). \quad (43)$$

Here we assume the Coulomb logarithm for a cluster of galaxy to be  $\ln \Lambda \approx 40$  (Suginohara & Ostriker 1998).

We use our theoretical results given by equation (13) for the mono-energetic diffusion reduction  $R_D = R_D(l_0/\lambda_L) = R_D(v^{-4}l_0/\lambda_{L,T})$  in the limits  $v^{-4}l_0/\lambda_{L,T} \ll 1$  and  $v^{-4}l_0/\lambda_{L,T} \gg 1$ ; and we use our numerical simulation results presented in Figure 3 for  $v^{-4}l_0/\lambda_{L,T} \sim 1$ . [We carry out the cubic spline interpolation of the simulation results. Note, that  $R_D$  is not differentiated in operator (29), so our final results are not sensitive to small noise errors in calculation of  $R_D$ .]

Using equations (39) and (42) with  $R_D$  given in Section 3, and numerically performing the velocity integrals, we find all four transport coefficients (41) normalized to the standard Lorentz coefficients (40). The dashed lines in Figures 5(a)–(h) show the resulting normalized transport coefficients  $\sigma$ ,  $\alpha$ ,  $\beta$  and  $\kappa$  as functions of  $l_0/\lambda_{L,T}$  for the two mirror spectra: (a) exponential, and (b) Gaussian [see equations (14)]. The asymptotic values of the coefficients at large values of  $l_0/\lambda_{L,T}$  are given by the numbers on the dashed lines, and they are unity. Thus, there is no reductions

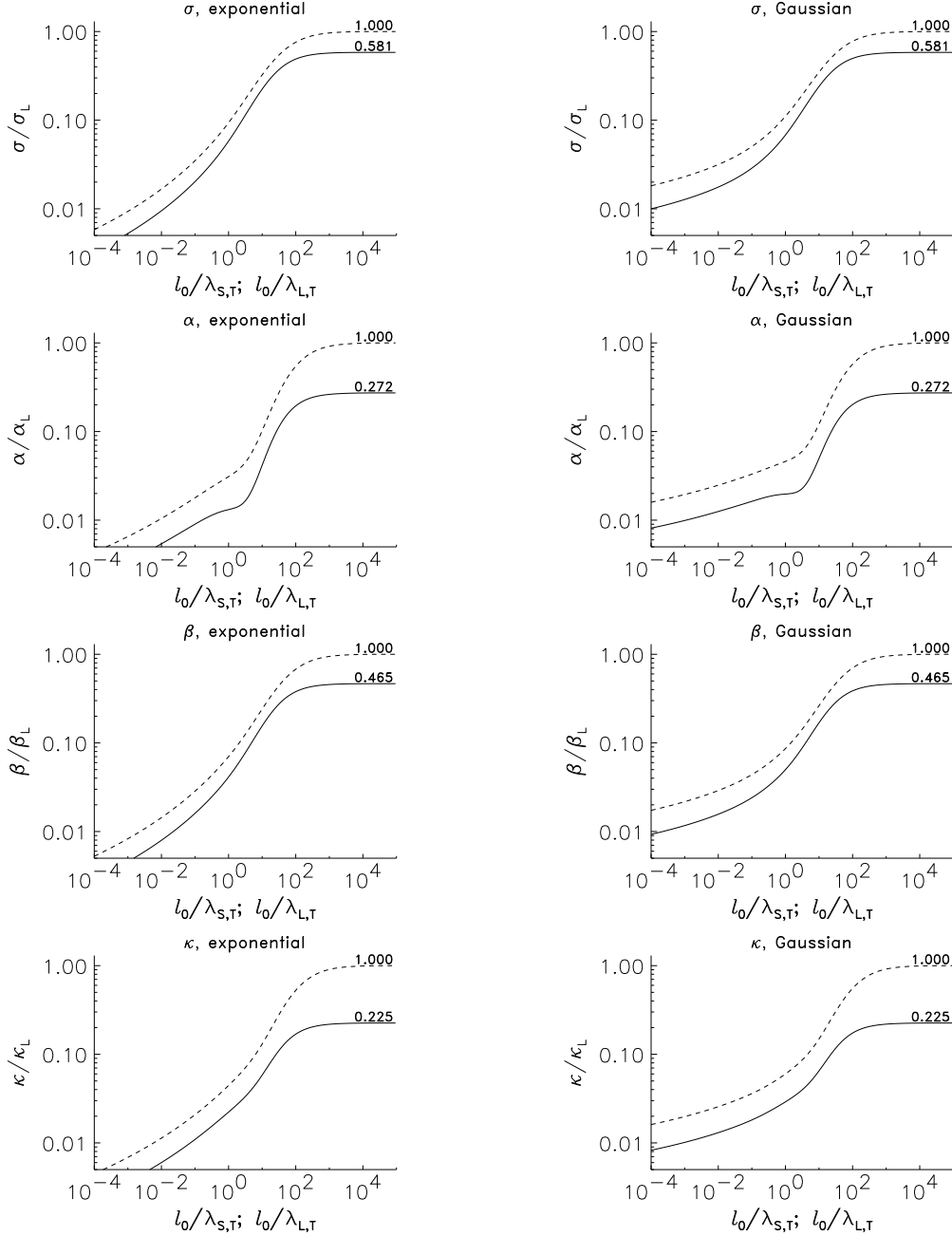


Fig. 5.— Figures on the left/right correspond to the exponential/Gaussian mirror spectra [see eqs. (14)]. The solid/dashed lines on all figures show the four transport coefficients,  $\sigma$ ,  $\alpha$ ,  $\beta$  and  $\kappa$ , for the Spitzer/Lorentz gas in the presence of stochastic magnetic mirrors as functions of the ratio of the magnetic field decorrelation length  $l_0$  to the Spitzer/Lorentz electron mean free path,  $\lambda_{S,T}/\lambda_{L,T}$ , calculated at the electron thermal speed  $V_T = \sqrt{2kT/m_e}$  [see eqs. (43), (46)]. All transport coefficients are normalized to the standard Lorentz transport coefficients given by equations (40). The asymptotic values of the coefficients at  $l_0/\lambda_T \gg 1$  are given by the numbers on the lines. They agree with the results of Spitzer & Härm (1953).



of the transport coefficients at  $l_0/\lambda_{L,T} \gg 1$ , as one can expect because there is no reduction of electron diffusivity in this limit [see equation (13)].

In a steady state, the electrical current  $j$  in a highly ionized plasma should be zero. Thus, if a temperature gradient is present, the resulting electric field  $E$  is obtained by setting  $j$  to zero in equation (34). Substituting this result for  $E$  into equation for the heat flow (35), we find for the effective thermal conductivity

$$\begin{aligned}\kappa_{\text{eff}} &= \kappa - \alpha\beta/\sigma, \\ \kappa_{\text{eff}}/\kappa_L &= \kappa/\kappa_L - (3/5)(\alpha/\alpha_L)(\beta/\beta_L)(\sigma_L/\sigma),\end{aligned}\tag{44}$$

where we use formulas (40) for the Lorentz transport coefficients in the second line of this equation.

Using the transport coefficients reported in Figures 5 by dashed lines and formula (44), it is easy to find the effective thermal conductivity  $\kappa_{\text{eff}}$  normalized to the standard Lorentz thermal conductivity  $\kappa_L$  [see equation (40)]. However, it is more useful to give the ratio of  $\kappa_{\text{eff}}$  to the Lorentz effective conductivity,  $\kappa_{L,\text{eff}} = 0.4\kappa_L$ . This ratio is the actual suppression of the effective conductivity of the Lorentz gas by magnetic mirrors. The dashed lines in Figures 6 show this suppression,  $\kappa_{\text{eff}}/\kappa_{L,\text{eff}}$ , as functions of  $l_0/\lambda_{L,T}$  for the two mirror spectra: (a) exponential, and (b) Gaussian [see equations (14)]. It has been estimated that the time of heat conduction in clusters of galaxies is possibly larger than the Hubble time if the thermal conductivity is less than 1/30 of the Spitzer value (Suginohara & Ostriker 1998). The horizontal dotted lines indicate this reduction of 1/30.

For comparison, the dotted lines represent the mono-energetic diffusion reduction at the electron thermal speed,  $R_D(l_0/\lambda_{L,T}) = D(l_0/\lambda_{L,T})/D_0$ . We see, that the Lorentz gas effective conductivity is reduced to a value two to three times smaller than that of the diffusion reduction. This is because heat is mainly transported by superthermal electrons. These electrons have long mean free paths, and the magnetic mirrors more strongly inhibit their diffusion.

## 5.2. Spitzer gas in a system of random mirrors

Now consider the full collision integral (28) for the Spitzer gas in a system of random magnetic mirrors. We have numerically solved the full set of our equations (29)–(32). The formulas (41) and (44) remain the same as for the Lorentz gas, but the functions  $S_T(v)$  and  $S_E(v)$  are different. For Spitzer electrons the mean free path is  $\lambda_S \propto V^4[1 + \Phi(v) - G(v)]^{-1}$  [Spitzer 1962, the error functions  $\Phi$  and  $G$  are given by (25)]. Thus, formula (42) for the reduction of spatial diffusivity now becomes

$$R_D = R_D(l_0/\lambda_S) = R_D\left(v^{-4} \frac{l_0}{\lambda_{S,T}} \frac{1 + \Phi(v) - G(v)}{1 + \Phi(1) - G(1)}\right),\tag{45}$$

where the Spitzer electron mean free at the thermal speed  $V_T = \sqrt{2kT/m_e}$  is

$$\lambda_{S,T} = 0.614 (kT)^2 / \pi n e^4 \ln \Lambda \approx 0.06 \text{ Kpc} (T/10^7 \text{ K})^2 (10^{-3} \text{ cm}^{-3}/n).\tag{46}$$

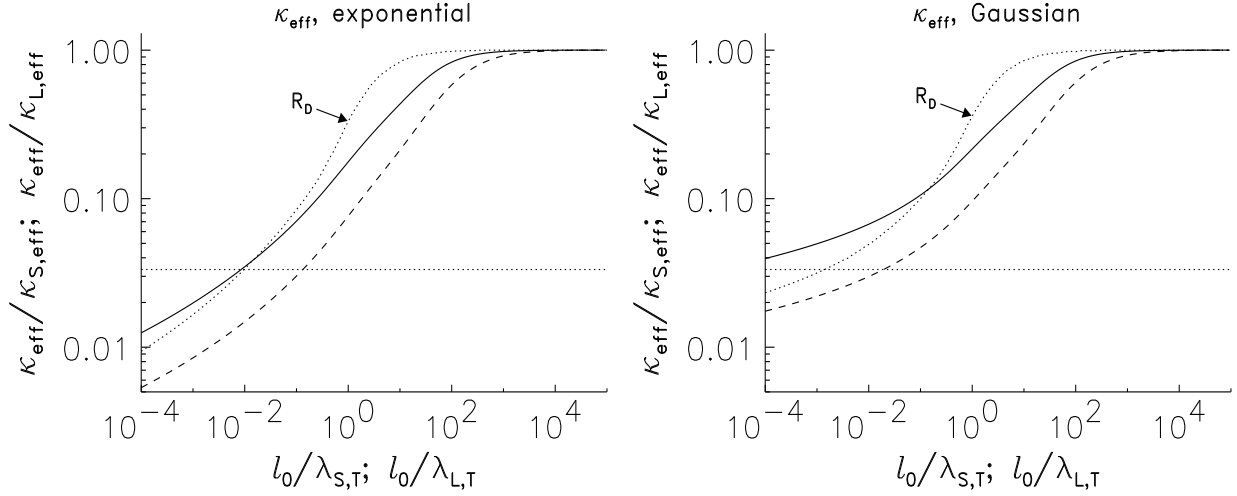


Fig. 6.— The solid/dashed lines show the reduction of the parallel effective thermal conductivity for the Spitzer/Lorentz gas by stochastic magnetic mirrors, as function of the ratio of the magnetic field decorrelation length to the Spitzer/Lorentz electron mean free path. The notations are the same as in Figure 5. For comparison, we give the mono-energetic diffusion reduction  $R_D(l_0/\lambda_T) = D(l_0/\lambda_T)/D_0$  by the dotted lines. The horizontal dotted lines represent the reduction of 1/30, below these lines the thermal conduction is so weak, that it should become negligible in clusters of galaxies.

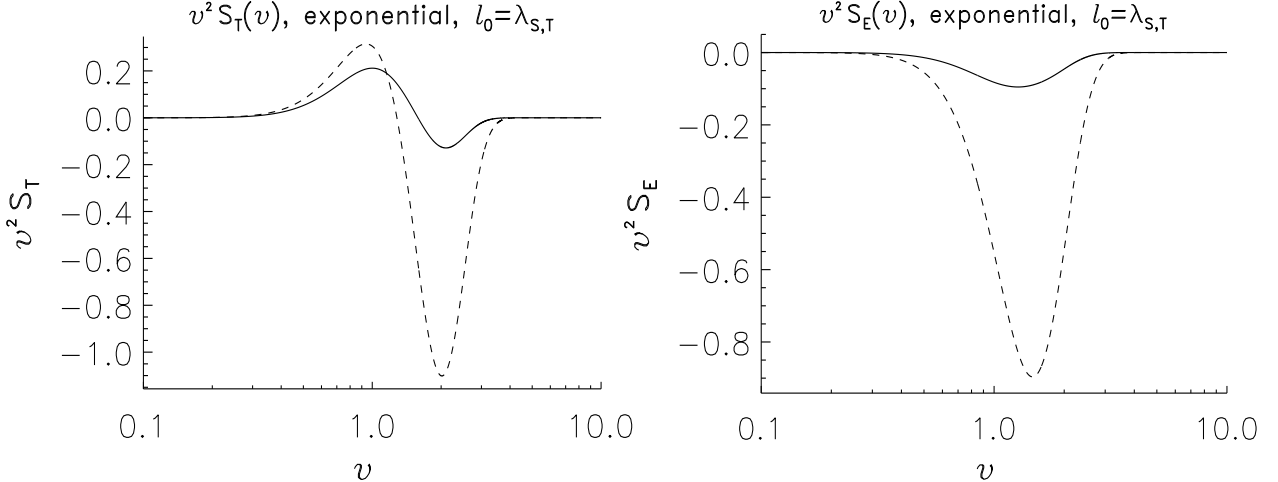


Fig. 7.— The solid lines show functions  $v^2 S_T(v)$  [the left figure] and  $v^2 S_E(v)$  [the right figure] for the Spitzer gas in a system of random magnetic mirrors for the case  $l_0 = \lambda_{\text{S,T}}$  [ $l_0$  is the magnetic field decorrelation length,  $\lambda_{\text{S,T}}$  is the Spitzer electron mean free path (46)]. The dashed lines in the corresponding plots show the same functions for the Spitzer gas without mirrors. Both graphs are plotted for the exponential mirror spectrum (for the Gaussian spectrum the results are similar).

Functions  $S_T(v)$  and  $S_E(v)$  are defined by equations (36), and they are the two inhomogeneous solutions of the equations (31), (32). To find these solutions we solved equation (31) numerically by iterations. At each iteration step the integral part of this equation,  $\hat{\mathcal{I}}S$ , was calculated using the solution for  $S$  from the previous step, and the new solution for  $S$  was calculated by the Gaussian decomposition with backsubstitution (Fedorenko 1994), using the boundary conditions (32). Initially, we started with zero function  $S = 0$ . The iterations converged very rapidly, and the Gaussian decomposition method is stable. We believe that our numerical method is much better and faster than the method of Spitzer and Härm (1953) because their method was not stable. It took us less than ten seconds of computer time to calculate all digits of the transport coefficients reported by Spitzer and Härm.

The solid lines in Figures 5(a)–(h) show the resulting transport coefficients  $\sigma$ ,  $\alpha$ ,  $\beta$  and  $\kappa$  normalized to the standard Lorentz coefficients (40) as functions of  $l_0/\lambda_{S,T}$  for the two mirror spectra: (a) exponential, and (b) Gaussian [see equations (14); remember that  $l_0$  is the magnetic field decorrelation length]. The asymptotic values of the coefficients at large values of  $l_0/\lambda_{S,T}$  are given by the numbers on the solid lines, and they agree with the results of Spitzer and Härm.

The effective thermal conductivity,  $\kappa_{\text{eff}}$ , normalized to the Spitzer effective conductivity,  $\kappa_{S,\text{eff}} = 0.0943 \kappa_L$ , is given in Figures 6 by the solid lines for the two mirror spectra. This normalized conductivity is the actual suppression of the effective thermal conductivity of the Spitzer gas by stochastic magnetic mirrors. *It is the result that should be applied in astrophysical problems with random magnetic mirrors.*

Finally, it is interesting to see how the mirrors change the Spitzer perturbed electron distribution function. In Figure 7 we plot functions  $v^2 S_T(v)$  and  $v^2 S_E(v)$  for the case when  $l_0 = \lambda_{S,T}$  [note that  $2\pi V^2 f_1$  is the actual distribution of electrons over speed  $V = vV_T$ , see equation (37)]. The solid lines represent these functions for the Spitzer gas in a system of random mirrors with the exponential mirror spectrum (for the Gaussian spectrum the results are similar). The dashed lines show the same functions for the Spitzer gas without magnetic mirrors. We see that  $v^2 S_T(v)$  and  $v^2 S_E(v)$  are reduced at large values of  $v$ , i.e. magnetic mirrors reduce the anisotropy of the superthermal electrons, which carry the electrical current and heat.

## 6. Conclusions

In this paper we have derived the actual parallel effective thermal conductivity that should be applied to astrophysical systems with random magnetic mirrors, as well as other important transport coefficients.

Now, let us apply our results for the reduction of the Spitzer effective electron thermal conductivity, shown in Figure 6 by the solid lines, to the galaxy cluster formation problem. If the reduction is by more than a factor of thirty (shown by the horizontal dotted lines in Figure 6), then the time of heat transport becomes larger than the Hubble time, and the heat conduction can be neglected (Suginohara & Ostriker 1998).<sup>7</sup> We see that this is the case if the magnetic field decorre-

---

<sup>7</sup>See the footnote on page 1.

lattice length  $l_0$  is roughly less than  $10^{-4} - 10^{-2}$  of the electron mean free path at the thermal speed  $\lambda_T = \lambda(\sqrt{2kT/m_e})$  (we consider the Spitzer gas). Although there is little observational data about the topology of magnetic fields in clusters of galaxy, the magnetic field scale is probably 1–10 Kpc (Kronberg 1994; Eilek 1999 and references in it). According to equation (46) the characteristic electron mean free path at the thermal speed is 0.06–60 Kpc for temperatures  $T = 10^7 - 10^8$  K and densities  $n = 10^{-4} - 10^{-3} \text{ cm}^{-3}$ . We see, that in general, the effective electron thermal conductivity parallel to the magnetic field lines is not reduced enough by magnetic mirrors to be completely neglected. However, as we pointed out in the introductory section, there is an additional effect that electrons have to travel along tangled magnetic field lines larger distances from hot to cold regions of space, so the thermal conduction is further reduced (this effect will be considered in our future paper). At the moment, “whether electron thermal conductivity in clusters of galaxies is sufficiently inhibited that it can be ignored” is still an open question.

Recently, Cowley, Chandran *et al.* studied the reduction of the parallel thermal conduction, and they concluded that the thermal conductivity in galaxy clusters is reduced enough to be neglected (Chandran & Cowley 1998; Chandran, Cowley & Ivanushkina 1999; Albright *et al.* 2000). Their conclusions are different from ours. The reason is that our approach in calculation of the conductivity is very different, and our results are qualitatively different. The main difference is that they took the reduction of thermal conductivity to be equal to the reduction of diffusivity of thermal electrons. In fact, the reduction of diffusivity is due to the enhanced pitch angle scattering by stochastic magnetic mirrors, and to find the reduction of thermal conductivity, the full set of kinetic equations must be derived and solved. This consistent way of solving the problem makes a considerable difference (see Figure 6). On the other hand, Cowley, Chandran and *et al.* first called attention to the importance of the effective mean free path  $\lambda_{\text{eff}}$  and found the correct qualitative result, that in the limit  $l_0 \ll \lambda$  the diffusion reduction is controlled by the mirrors whose spacing is of order of the effective mean free.

We are happy to acknowledge many useful discussions of this problem with Jeremiah Ostriker, Jeremy Goodman and David Spergel. We would also like to thank Makoto Matsumoto, Takuji Nishimura and Shawn J. Cokus providing us with fast random number generators (which are given at <http://www.math.keio.ac.jp/matsumoto/emt.html>). This work was partially supported by DOE under Contract No. DE-AC 02-76-CHO-3073. Leonid Malyskin would also like to thank the Department of Astrophysical Sciences at Princeton University for financial support.

### A. Solution of equation (3) in the limit $l_m \ll \lambda_{\text{eff}}$

Here we solve equation (3) by expansion in the limit  $l_m \ll \lambda_{\text{eff}}$ . This condition means that collisions are too weak to scatter the electron out of the loss cones. Therefore,  $F(x, \mu) \equiv 0$  when  $|\mu| > \mu_{\text{crit}}$ .

We make use the fact that  $(V/\nu)(\partial/\partial x) \sim \lambda/l_m \gg 1$ . Also we will show that  $1/\nu\tau_m \ll 1$ . The validity of this last assumption appears below. To zero order, we have  $\partial F/\partial x = 0$ , and  $F(x, \mu) = F_0(\mu)$ .  $F_0(-\mu) = F_0(\mu)$  because of electron reflection at the mirrors and the symmetry

of the loss cones. Up to first order,  $F(x, \mu) = F_0(\mu) + F_1(x, \mu)$ , and we have

$$\mu V \frac{\partial F_1}{\partial x} = \frac{\nu}{2} \frac{\partial}{\partial \mu} \left[ (1 - \mu^2) \frac{\partial F_0}{\partial \mu} \right] + \frac{F_0}{\tau_m}. \quad (\text{A1})$$

We integrate this equation over  $x$  along a closed back and forth trajectory of a trapped electron shown by the dotted lines in Figure 1(b), to obtain

$$\begin{cases} \partial/\partial \mu [(1 - \mu^2) \partial F_0 / \partial \mu] + 2F_0 / \nu \tau_m = 0, \\ F_0(-\mu) = F_0(\mu), \quad F_0(\pm \mu_{\text{crit}}) = 0. \end{cases} \quad (\text{A2})$$

We solve equation (A2) by a further expansion,  $1/\nu\tau_m \ll 1$ . The even solution in the “inside” region  $1 - |\mu| \gg e^{-\nu\tau_m}$  up to first order is

$$F_0^{(i)} = C^{(i)} \left[ 1 - \frac{1}{\nu\tau_m} \ln \frac{1}{1 - \mu^2} \right], \quad 1 - |\mu| \gg e^{-\nu\tau_m}. \quad (\text{A3})$$

On the other hand, the zero order solution in the “boundary” regions  $1 - |\mu| \ll 1$  is

$$F_0^{(b)} = C^{(b)} \ln \frac{1 - |\mu|}{1 - \mu_{\text{crit}}}, \quad 1 - \mu_{\text{crit}} \leq 1 - |\mu| \ll 1. \quad (\text{A4})$$

We match solutions (A3) and (A4) together in regions  $e^{-\nu\tau_m} \ll 1 - |\mu| \ll 1$  to finally obtain  $\tau_m = \nu^{-1} \ln m$ , justifying  $1/\nu\tau_m \ll 1$ . This is the first result in equation (5).

## B. Solution of equation (3) in the limits $\lambda_{\text{eff}} \ll l_m \ll \lambda^2/\lambda_{\text{eff}}$ and $\lambda^2/\lambda_{\text{eff}} \ll l_m$

Let us consider the kinetic equation (3) in the more limited case  $\lambda \ll l_m$  (note that  $\lambda_{\text{eff}} \ll \lambda$ ). This means that in the kinetic equation  $(V/\nu)(\partial/\partial x) \lesssim \lambda/l_m \ll 1$ . We will also show that  $1/\nu\tau_m \ll 1$ . The validity of this assumption appears below. To zero order, we have  $\partial F/\partial \mu = 0$ , so  $F(x, \mu) = F_0(x)$ .  $F_0(-x) = F_0(x)$  because of symmetry. Up to first order,  $F(x, \mu) = F_0(x) + F_1(x, \mu)$ , and we have

$$\frac{\nu}{2} \frac{\partial}{\partial \mu} \left[ (1 - \mu^2) \frac{\partial F_1}{\partial \mu} \right] = \mu V \frac{\partial F_0}{\partial x} - \frac{F_0}{\tau_m}. \quad (\text{B1})$$

We integrate the above equation over  $\mu$ , and then set  $\mu = \pm 1$  to find the constant of integration. As a result, we obtain  $F_0/\tau_m \ll V(\partial F_0/\partial x)$  [so,  $1/\nu\tau_m$  is of second order], and  $\partial F_1/\partial \mu = -(V/\nu)(\partial F_0/\partial x)$ . We integrate this last equation over  $\mu$  once more, and obtain

$$F_1 = -(\mu V/\nu)(\partial F_0/\partial x) + C(x), \quad (\text{B2})$$

where  $C(x)$  is another integration constant.

We continue the expansion of the kinetic equation (3) to next order. Up to second order,  $F(x, \mu) = F_0(x) + F_1(x, \mu) + F_2(x, \mu)$ . Using equation (B2), we have

$$\frac{\nu}{2} \frac{\partial}{\partial \mu} \left[ (1 - \mu^2) \frac{\partial F_2}{\partial \mu} \right] = -\frac{\mu^2 V^2}{\nu} \frac{\partial^2 F_0}{\partial^2 x} + \mu V \frac{\partial C}{\partial x} - \frac{F_0}{\tau_m}. \quad (\text{B3})$$

We integrate equation (B3) over  $\mu$  from  $-1$  to  $1$  and obtain

$$\begin{cases} \partial^2 F_0 / \partial^2 x + (3\nu/\tau_m V^2) F_0 = 0, \\ F_0(-x) = F_0(x). \end{cases} \quad (\text{B4})$$

Finally, we integrate this equation and obtain zero order solution for the time-dependent distribution function (2)

$$f(t, x) = e^{-t/\tau_m} F_0(x) = e^{-t/\tau_m} \cos\left(x\sqrt{3\nu/\tau_m V^2}\right), \quad (\text{B5})$$

where we drop an unnecessary normalization constant of integration.

Now, to find  $\tau_m$ , we calculate the flux of escaping electrons through the two escape windows (see Figure 1)

$$\partial N / \partial t = -2 \int_{\mu_{\text{crit}}}^1 \mu V f(t, l_m/2) d\mu = -(V/m) e^{-t/\tau_m} \cos\left[(l_m/2)\sqrt{3\nu/\tau_m V^2}\right], \quad (\text{B6})$$

where we use equation (B5) for  $f(t, l_m/2)$ . On the other hand, the flux is equal to the change of the total number of electrons

$$\partial N / \partial t = \int_{-l_m/2}^{l_m/2} \int_{-1}^1 (\partial f / \partial t) d\mu dx = -(4/\tau_m) e^{-t/\tau_m} \sqrt{\tau_m V^2 / 3\nu} \sin\left[(l_m/2)\sqrt{3\nu/\tau_m V^2}\right]. \quad (\text{B7})$$

Equating the two formulas for  $\partial N / \partial t$ , we obtain

$$(3/16)(\nu\tau_m/m^2) = \tan^2\left(\sqrt{3\nu l_m^2 / 4\tau_m V^2}\right). \quad (\text{B8})$$

In the limit  $\lambda \ll l_m \ll \lambda^2/\lambda_{\text{eff}}$  the argument of the tangent above is small, so we expand the tangent and obtain  $\tau_m = \nu^{-1}(l_m/\lambda_{\text{eff}})$ , while  $F_0 \approx \text{const}$ . In the limit  $\lambda^2/\lambda_{\text{eff}} \ll l_m$  the left hand side of equation (B8) is large, therefore, the argument of the tangent is  $\pi/2$ , and we have  $\tau_m = \nu^{-1}(3/\pi^2)(l_m/\lambda)^2$  [the third line in equation (5)], i.e. the escape time is controlled by diffusion in  $x$ -space. In both limits  $1/\nu\tau_m \ll 1$ , as we assumed above, (and of second order).

Now, the limit  $\lambda_{\text{eff}} \ll l_m \lesssim \lambda$  is still left. The result in this case is the same as the result in case  $\lambda \ll l_m \ll \lambda^2/\lambda_{\text{eff}}$ . However, instead of solving the kinetic equation, we give the following qualitative arguments supported by our numerical simulations (see Figure 2). The relaxation time of the electron distribution in  $\mu$ -space can be estimated as  $\Delta t_\mu \sim \nu^{-1}$ . The relaxation time in  $x$ -space can be estimated as the crossing time  $\Delta t_x \sim l_m/V = \nu^{-1}(l_m/\lambda)$  in case  $l_m \lesssim \lambda$ , and as the time of diffusion across  $\Delta t_x \sim \nu^{-1}(l_m/\lambda)^2$  in case  $\lambda \ll l_m$ . All relaxation times are small compared to the escape time  $\tau_m$ , i.e.  $\Delta t_\mu, \Delta t_x \ll \tau_m$  for the entire range  $\lambda_{\text{eff}} \ll l_m \ll \lambda^2/\lambda_{\text{eff}}$ . This means that the distribution function is approximately constant in  $x$  and  $\mu$ , say  $F_0 \approx 1$ ,  $f \approx e^{-t/\tau_m}$ . We then carry out calculations similar to those we used in formulas (B6) and (B7) to find that  $\tau_m = \nu^{-1}(l_m/\lambda_{\text{eff}})$  [the second line in equation (5)].

### C. The Additional electron flow produced by electric field

Let us, for simplicity, consider the Lorentz gas. The results for the Spitzer gas are similar.

First, we derive an estimate for the additional flow  $d\tilde{\mathcal{F}}$  of electrons that are in an interval  $V \in [V, V + dV)$  of the velocity space, produced by an electric field  $E$  due to the change of the two loss cones of a mirror trap. Let us consider only the principle mirrors, because they mainly control the diffusion of electrons (see Section 3). In this appendix, we denote their mirror strength (the principle mirror strength) as  $M$ .

The principle mirror strength is of order of five, so in the case when the magnetic field decorrelation length is more than or approximately equal to the electron mean free path,  $l_0 \gtrsim \lambda$ , the escape of electrons from the mirror trap is mainly controlled by their spatial diffusion, see Section 2. Thus, in this limit, the electrons “do not care” about the size of the loss cones, and therefore, no additional flow arises.

In the case  $l_0 \lesssim \lambda$  there is a non-zero additional flow  $d\tilde{\mathcal{F}}$ . In Figure 1(b), because of the electric field, the loss cone on the left,  $\mu_{\text{crit},-}$ , is not equal to that on the right,  $\mu_{\text{crit},+}$ . The size of the two loss cones is estimated from the conservation of the electron magnetic moment,  $(1 - \mu^2)V^2/B = \text{const}$ , and from the conservation of energy,  $m_e V^2/2 + eEx = \text{const}$ . We have

$$\mu_{\text{crit},\pm}^2 \approx 1 - 1/M \pm (eEl_M/m_e V^2 M), \quad (\text{C1})$$

where  $l_M$  is the spacing of the principle mirrors.

Let  $d\tilde{\mathcal{F}}_+$  and  $d\tilde{\mathcal{F}}_-$  be the absolute values of the fluxes of the escaping electrons to the right and to the left respectively. Then, their sum is

$$d\tilde{\mathcal{F}}_+ + d\tilde{\mathcal{F}}_- = (l_M/\tau_M) 2\pi V^2 f_0 dV, \quad (\text{C2})$$

where  $2\pi V^2 f_0 dV$  is the number density of electrons expressed in terms of the Maxwellian zero order electron distribution function  $f_0$ , and  $\tau_M$  is the escape time, see equations (2), (6), (16) and Section 2. The actual electron flow,  $d\tilde{\mathcal{F}}$ , is equal to the difference of  $d\tilde{\mathcal{F}}_+$  and  $d\tilde{\mathcal{F}}_-$ , because they are in opposite directions. An estimate for the ratio  $d\tilde{\mathcal{F}}/(d\tilde{\mathcal{F}}_+ + d\tilde{\mathcal{F}}_-)$  is

$$\frac{d\tilde{\mathcal{F}}}{d\tilde{\mathcal{F}}_+ + d\tilde{\mathcal{F}}_-} = \frac{d\tilde{\mathcal{F}}_+ - d\tilde{\mathcal{F}}_-}{d\tilde{\mathcal{F}}_+ + d\tilde{\mathcal{F}}_-} \approx \left[ \int_{\mu_{\text{crit},+}}^1 \mu d\mu - \int_{\mu_{\text{crit},-}}^1 \mu d\mu \right] / \left[ \int_{\mu_{\text{crit},+}}^1 \mu d\mu + \int_{\mu_{\text{crit},-}}^1 \mu d\mu \right]. \quad (\text{C3})$$

Now, using equations (C1)–(C3), we obtain the additional electron flow

$$d\tilde{\mathcal{F}} \approx -2\pi(eE/m_e) f_0 (l_M^2/\tau_M) dV. \quad (\text{C4})$$

The factor  $(l_M^2/\tau_M)$  in this equation is proportional to the spatial diffusivity of the electrons (provided that the diffusivity is controlled by the principle mirrors, see Section 3). Thus, it is obviously  $l_M^2/\tau_M = R_D \lambda_L^2 \nu_L$ , where  $\lambda_L$  and  $\nu_L$  are the standard Lorentz mean free path and collision frequency, and  $R_D$  is the reduction of the spatial diffusivity reported in Section 3. Using that  $\lambda_L \propto V^4$ ,  $\nu_L \propto V^{-3}$ , and equations (16), (43),  $V_T = \sqrt{2kT/m_e}$ , we finally obtain

$$d\tilde{\mathcal{F}} \approx -(1/2)(2/\pi)^{3/2} \left( k^{3/2} T^{3/2} E / m_e^{1/2} e^3 \ln \Lambda \right) R_D v^5 e^{-v^2} dv. \quad (\text{C5})$$

Now we like to compare this result for the additional flow  $d\tilde{\mathcal{F}}$  with the main flow  $d\mathcal{F}$  produced by the electric field due to acceleration of particles. The later is

$$d\mathcal{F} = \int_{-1}^1 \mu V f_1 d\mu 2\pi V^2 dV d\mu = -(2/3)(2/\pi)^{3/2} \left( k^{3/2} T^{3/2} E / m_e^{1/2} e^3 \ln \Lambda \right) R_D v^7 e^{-v^2} dv, \quad (\text{C6})$$

where we substituted function  $f_1$  given by (17), and function  $S(v) = \gamma_E S_E(v)$  given by (33) and (39). As a result,

$$d\tilde{\mathcal{F}}/d\mathcal{F} \approx (3/4) v^{-2}. \quad (\text{C7})$$

Because the electrical current and the heat flow are mainly transported by superthermal electrons  $v^2 \sim 4$ , the additional flow produced by electric field due to non-equal loss cones can indeed be neglected in comparison with the main flow due to acceleration of electrons by electric field.

## REFERENCES

- Albright, B. J., Chandran, B. D. G., Cowley, S. C., & Loh, M., 2000, in press
- Braginskii, S. I., 1965, *Rev. of Plasma Phys.*, **1**, 205.
- Cen, R., & Ostriker, J., 1999, *ApJ*, **514**, 1
- Chandran, B. D. G., & Cowley, S. C., 1998, *Phys. Rev. Lett.*, **80**, 3077
- Chandran, B. D. G., Cowley, S. C., & Ivanushkina, M., 1999, *ApJ*, **525**, 638
- Cohen, R. S., Spitzer Jr, L., & Routly, P. McR., 1950, *Phys. Rev.*, **80** (2), 230
- Eilek, J., 1999, astro-ph/9906485, *Diffuse Thermal and Relativistic Plasma in Galaxy Clusters*, 1999 Ringberg Workshop, Germany, (in press)
- Fabian, A. C., 1990, *Physical Processes in Hot Cosmic Plasmas*, 271, NATO ASI Series, Netherlands: Kluwer Acad. Publishers
- Fedorenko, R. P., 1994, *Introduction into computational physics*, Moscow: Moscow Institute of Physics and Technology Press
- Kronberg, P. P., 1994, *Rep. Prog. Phys.*, **57**, 325
- Pistinner, S., & Shaviv, G., 1996, *ApJ*, **459**, 147
- Rosenbluth, M. N., MacDonald W. M., & Judd, D. L., 1957, *Phys. Rev.*, **107** (1), 1
- Rosner, R., & Tucker, W. H., 1989, *ApJ*, **338**, 761
- Spitzer Jr, L., 1962, *Physics of fully ionized gases*, New York: Wiley
- Spitzer Jr, L., & Härm, R., 1953, *Phys. Rev.*, **89** (5), 977



Suginohara, T., & Ostriker, J., 1998, ApJ, **507**, 16

Tao, L., 1995, MNRAS, **275**, 965

Tribble, P. C., 1989, MNRAS, **238**, 1247